12th IMEKO TC4 International Symposium
Electrical Measurements and Instrumentation
September 25–27, 2002, Zagreb, Croatia

MEASUREMENT ACCURACY OF FILTER BANK BASED ADC BUILT IN SELF TEST

Chiheb Rebai, Dominique Dallet and Philippe Marchegay

Laboratoire de Microélectronique IXL-ENSEIRB, Université Bordeaux I, France
Email: rebai, dallet, marchegay@ixl.u-bordeaux.fr

Abstract − In this paper, we present the analysis of Built-In-Self-Test (BIST) scheme for Analogue to Digital Converter (ADC). This work focuses on a filter bank based BIST for power spectral density measurement. Digital filter structure will be used to decompose the ADC output signal into its main spectral components. Numerical simulations are conducted to validate our idea and the results show that the scheme is a promising BIST approach for ADC.

Keywords: ADC, BIST, Filter bank.

1. INTRODUCTION

The demand for higher quality, performance, and ease of maintenance ADCs, all at a lower cost, keeps on growing. Manufacturers are searching for ways to deliver ADC with greater resolution and speed at ever more economical prices. One of the key factors for this kind of success is low-cost, highly accurate testing. Until now, the semiconductor industry has relied mostly upon the use of sophisticated, high-speed ADC test setup to minimize the test time for each chip as it pass through the test phase of the manufacturing process. The inclusion of BIST (Built In Self Test) capabilities at the chip level will reduce the requirement for high performance test equipment at every stage in the manufacturing process: chip, board, system, and field service. In this paper, we present a BIST scheme, based on digital filtering, by which the power spectral density of the ADC output data can be performed.

In the first part of this paper, we recall the three major methods for the ADC characterisation: time domain analysis, statistical analysis, and spectral analysis. The proposed BIST structure, described in the second part of the paper, performs the separation of ADC output signal in his main spectral components (harmonics and noise). The accuracy of the proposed method will be compared to measurement made by FFT in the third part. In the last section, simulation results and implementation considerations are presented to validate the accuracy of the proposed structure.

2. THE CLASSICAL ADC TEST AND MEASUREMENT

The ADC is the major component linking the analogue word to the numerical one. This conversion reduces the quality of the analogue signal which is converted in a numerical form. It is therefore important to measure the systematic error and defects introduced by the analogue to digital conversion.

Three methods are available for this task [1]. The industry standard is the Fast Fourier Transform (FFT) which performs the analysis within the frequency domain. The FFT method gives a wider number of parameters about the ADC but it requires a large amount of resources and is not always suitable for on chip implementation. The sine wave fitting method presents a great advantage of not being exigent in terms of coherent sampling. The use of this method in BIST is recommended only if the number of frequency components of interest is small. The histogram method makes a statistical analysis and the large number of samples is a serious disadvantage for on chip implementation.

3. THE PROPOSED ADC TEST METHOD

An alternative method to analyze the digital data from the ADC is digital filtering. The principle consists in conceiving a system that provides the spectral components of a signal. The system is a network of second order filter. Each cell extracts one tone (fundamental or harmonic) [2].

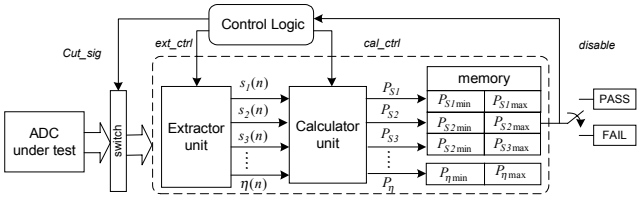

Fig. 1. The proposed structure

Fig. 1 depicts the proposed architecture. The required circuitry includes control logic (to generate control signals), the extractor unit, the calculator unit, memory (to compare the calculated and the stored results) and the analog switches surrounding the ADC.

3.1. The extractor Unit

3.1.1 Second order band pass filter

The bandpass LDI (Lossless Digital Integrator) filter is derived from bilinearly transformed second order continuous time transfer function. In [2] authors present an IIR bandpass filter that has exactly unity gain and zero

phase shift at resonance. This structure is preferable for applications where the signals are at frequency much less than the sampling frequency.

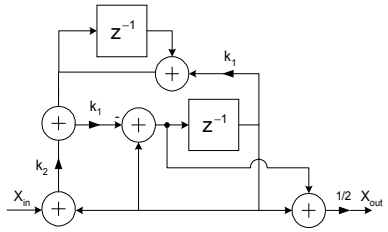

Fig. 2. The second order bandpass filter

The transfer function from the input to the bandpass output is given by

$$H_{bp}(z) = \frac{-k_2}{2} \times \frac{(1+z^{-1})(1-z^{-1})}{1-(2-k_2-k_1^2)z^{-1}+(1-k_2)z^{-2}} \quad (1)$$

This transfer function has a peak gain of exactly unity at the frequency given by

$$f_r = \frac{1}{\pi}\sin^{-1}\left(k_1 \Big/ 2\sqrt{1-\frac{k_2}{2}}\right) \quad (2)$$

3.1.2 Notch filter

The case of tracking a single sinusoid is shown schematically in Fig. 3. A notch filter is obtained when the output of the bandpass filter is subtracted from its input. The enhaced sinusoid is avaiblable at the output of the bandpass filter for detection and characterisation.

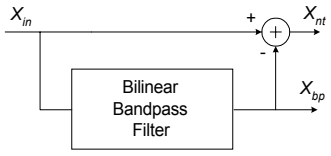

Fig. 3. The notch filter

3.1.3 Notch filter bank

When tracking multiples sinusoids, a cascade structure is recommended. The overall filter is shown in Fig. 4.

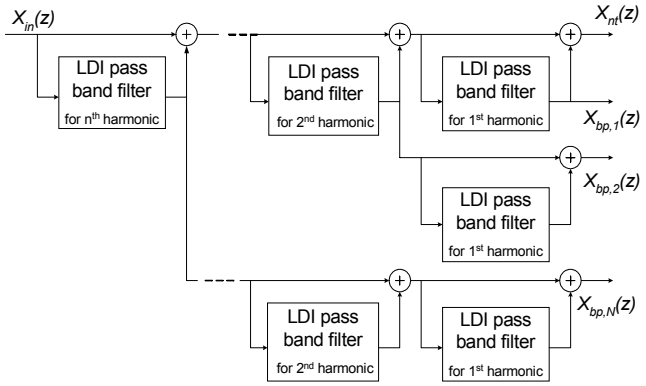

Fig. 4. The notch filter bank

This structure requires $N(N+1)/2+N$ biquads for tracking N sinusoids. This structure has a number of specific features in comparison with others cascade or parallel implementations described in recent literature [3]. The transfer function from the filter input to these nodes will have close to unity gain at the frequency of the sinusoid being isolated and transmission zeros at all other sinusoids.

3.2 The Calculator unit

3.2.1 Theorical background

The digital notch filter bank, presented in Fig. 4, is connected to the output of the ADC as shown in Fig. 1. Let $y(n)$ be the digital sequence applied to the filter input X_{in}. The signals s_i and η will denote the digital code emerging from the bandpass output $X_{bp,i}$ and the notch output X_{nt}, respectively. Since the sequence $s_i(n)$ emerging from the bandpass output is zero-mean, the estimated power $\hat{P}_s$ is computed as a sum of squares, given by (3) where M in the number of samples.

$$\hat{P}_{s,i} = \frac{1}{M-1}\sum_{n=1}^{M}(s_i(n))^2 \quad (3)$$

The sequence $\eta(n)$ emerging from the notch output X_{nt} is not zero-mean so it variance, which is the estimated noise power $\hat{P}_\eta$, is calculated as

$$\hat{P}_\eta = \frac{1}{M-1}\sum_{n=1}^{M}(\eta(n))^2 - \frac{\left(\sum_{n=1}^{M}\eta(n)\right)^2}{M(M-1)} \quad (4)$$

3.2.2 Implementation consideration

To determinate the noise power and the signal power we use a combinaison of multiplier, adders, registers and gain. Fig. 5 and Fig. 6 detail, respectivly, the signal and the noise powers calculations.

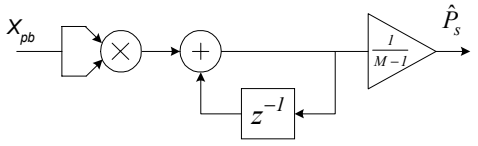

Fig. 5. Signal power calculation

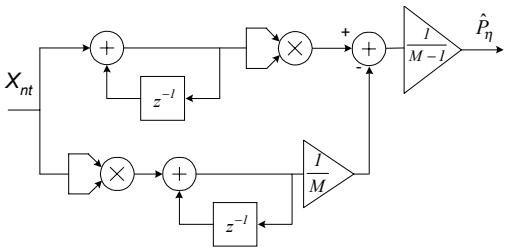

Fig. 6. Noise power calculation

4. ACCURACY OF MEASUREMENT

We are interested in performing measurements on physical circuits. The output of the ADC circuit will contain a finite amount of random noise no matter how clean and precise the applied stimulus. Therefore, the measurements discussed in the previous section are executed in the presence of random noise. Consequently, the measurement results themselves will exhibit some degree of randomness

due to the noise. Each time the frequency response measurement is repeated on the same ADC under the same conditions, the results will all be slightly different from each other but will be within a certain range. We must ensure that this random deviation between test outcomes is much less than the desired accuracy of the test.

4.1 Precision via FFT

As we mentioned at the beginning of the section, whenever a signal is measured in the presence of white noise, some of the noise power will be at the same frequency of the signal. The result is that when a measurement is made which uses FFT on the sum of the signal plus noise (ADC output), the measurement results will exhibit random variation due to the effect of the white noise. Utilising previous results, we will now develop a bound on the amount of variation observed in the measured signal power extracted via an FFT on ADC output represented by the the sum of the signal plus white noise.

4.1.1 PDF of FFT of Gaussien Noise

Let us begin with a sequence of M samples of Gaussan white noise $\eta(n)$. We will assume that the random noise is zero-mean and that all samples are independent, and identically distributed with a standard of σ_η. The FFT $N(k)$ of the noise $\eta(n)$ is computed from

$$N(k)=\sum_{i=0}^{M-1}\eta(i)e^{-j\frac{2\pi}{M}ki},\quad k=0,...,M-1 \tag{5}$$

Expanding to obtain the real and imaginary parts in

$$\begin{aligned} N(k) &= \mathrm{Re}[N(k)]+j\,\mathrm{Im}[N(k)] \\ &= \sum_{i=0}^{M-1}\eta(i)(\cos(2\pi ik/M)-j\sin(2\pi ik/M)) \\ &= \sum_{i=0}^{M-1}\eta(i)\cos(2\pi ik/M)-j\sum_{i=0}^{M-1}\eta(i)\sin(2\pi ik/M) \end{aligned} \tag{6}$$

We notice that the real and imaginary parts of $N(k)$ are each linear combinations of Gaussian random variables. N is expressed in $Volts/\sqrt{Hz}$. Therefore, the real and imaginary parts of $N(k)$ will also be Gaussian (Central Limit theorem) [4].

Computing the mean for the real and imaginary parts separately, we obtain

$$E\{\mathrm{Re}[N(k)]\}=\sum_{i=0}^{M-1}E\{\eta(i)\cos(2\pi ik/M)\}=0 \tag{7}$$

$$E\{\mathrm{Im}[N(k)]\}=-\sum_{i=0}^{M-1}E\{\eta(i)\sin(2\pi ik/M)\}=0 \tag{8}$$

where $E\{x\}$ is the mean value of the random variable x. The variance v for the real and imaginary parts of the sum is found in the same way:

$$\begin{aligned} v\{\mathrm{Re}[N(k)]\} &= \sum_{i=0}^{M-1}v\{\eta(i)\cos(2\pi ik/M)\} \\ &= \sigma_\eta^2\sum_{i=0}^{M-1}\cos^2(2\pi ik/M) \\ &= \sigma_\eta^2 M/2 \end{aligned} \tag{9}$$

$$\begin{aligned} v\{\mathrm{Im}[N(k)]\} &= -\sum_{i=0}^{M-1}v\{\eta(i)\sin(2\pi ik/M)\} \\ &= \sigma_\eta^2\sum_{i=0}^{M-1}\sin^2(2\pi ik/M) \\ &= \sigma_\eta^2 M/2 \end{aligned} \tag{10}$$

4.1.2 PDF of FFT of signal plus White noise

Consider adding a sine wave $x(n)$ to the noise such that the sine wave has exactly m number of complete cycles in M samples. That is,

$$x(n)=A_x\sin(2\pi mn/M+\phi_x) \tag{11}$$

where n=0,… M-1, Φ_x is constant and m is integer. The FFT of the $x(n)$ will be

$$X(k)=\begin{cases} A_x(M/2)\sin(\phi_x)-jA_x(M/2)\cos(\phi_x), & pour\ k=m \\ A_x(M/2)\sin(\phi_x)+jA_x(M/2)\cos(\phi_x), & pour\ k=M-m \\ 0, & sinon \end{cases} \tag{12}$$

Note that since $x(n)$ is fully deterministic, the PDF for the real and imaginary parts of $X(k)$ will simply be unit impulses at the appropriate values of $X(k)$. Furthermore, the real and imaginary parts of $X(k)$ will be the means μ_R and μ_I, respectively, of the real and imaginary parts of the FFT of the signal plus noise, as we shall see. Let $y(n)=x(n)+\eta(n)$ be the sum of the signal plus noise which represent the ADC output. Computing M-point FFT, we obtain

$$Y(k)=X(k)+N(k) \tag{13}$$

The real and imaginary parts of $Y(k)$ in the frequency bins $k=m$ and $k=M-m$ will be Gaussian. Their means μ_R and μ_I will be equal to the real and imaginary parts of $X(m)$ et $X(M-m)$. All frequency bins $Y(k)$, $k=0,...M-1$ will have equal variance $\sigma_\eta^2 M/2$. Thus having the mean variance of the signal plus noise in the frequency bins and knowing that PDF is Gaussian, we able to compute the confidence intervals. The 95% confidence interval for the real and imaginary parts of $Y(k)$ is

$$\begin{Bmatrix} A_x(M/2)\sin(\phi_x)-2\sigma_\eta\sqrt{M/2}, & for\ k=m,M-m \\ -2\sigma_\eta\sqrt{M/2}, & otherwise \end{Bmatrix} \le \mathrm{Re}[Y(k)] \le \begin{Bmatrix} A_x(M/2)\sin(\phi_x)+2\sigma_\eta\sqrt{M/2}, & for\ k=m,M-m \\ 2\sigma_\eta\sqrt{M/2}, & otherwise \end{Bmatrix} \tag{14}$$

$$\begin{Bmatrix} -A_x(M/2)\cos(\phi_x)-2\sigma_\eta\sqrt{M/2}, & for\ k=m \\ A_x(M/2)\cos(\phi_x)-2\sigma_\eta\sqrt{M/2}, & for\ k=M-m \\ -2\sigma_\eta\sqrt{M/2}, & otherwise \end{Bmatrix} \le \mathrm{Im}[Y(k)] \le \begin{Bmatrix} -A_x(M/2)\cos(\phi_x)+2\sigma_\eta\sqrt{M/2}, & for\ k=m \\ A_x(M/2)\cos(\phi_x)+2\sigma_\eta\sqrt{M/2}, & for\ k=M-m \\ 2\sigma_\eta\sqrt{M/2}, & otherwise \end{Bmatrix} \tag{15}$$

We will determine the PDF of Y_m^2, and then proceed to an approximate PDF of S_m. The sum of squares of the real and imaginary parts of $Y(m)$ is $|Y(m)|^2=Y_m^2$. This situation satisfies the criteria for non-central chi squared PDF with 2

degree of freedom [5]. The random variable Y_m^2 has a PDF given by

$$p\left(Y_m^2\right)=\frac{1}{2\sigma^2}e^{-\left(\mu_R^2+\mu_I^2+Y_m^2\right)}I_0\left(\frac{\sqrt{Y_m^2\left(\mu_R^2+\mu_I^2\right)}}{2\sigma^2}\right),\quad Y_m^2\geq 0 \tag{16}$$

The term $I_0(x)$ is a zero-th order Bessel function of the first kind, which may be represented by the infinite series

$$I_0(x)=\sum_{k=0}^{\infty}\frac{(x/2)^{2k}}{k!\,\Gamma(k+1)},\quad x\geq 0 \tag{17}$$

where $\Gamma(p)$ is the gamma function, defined as

$$\Gamma(p)=\int_0^{\infty}t^{p-1}e^{-t}dt,\quad p\geq 0 \tag{18}$$

Assuming that at least one of either μ_R and μ_I is non-zero, the mean and variance of Y_m^2 are

$$\mu_{Y_m^2}=2\sigma^2+\mu_R^2+\mu_I^2=M\sigma_\eta^2+\left(\mu_R^2+\mu_I^2\right) \tag{19}$$

$$\sigma_{Y_m^2}^2=4\sigma^2+4\sigma^2\left(\mu_R^2+\mu_I^2\right)=M^2\sigma_\eta^4+2\sigma_\eta^2M\left(\mu_R^2+\mu_I^2\right) \tag{20}$$

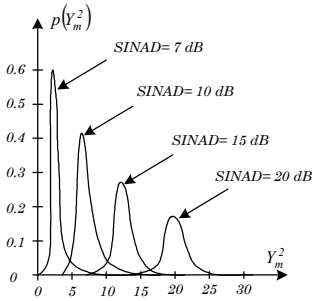

Fig. 7. The PDF of the FFT bins which contains Y_m^2 for various SINAD

As μ_R and μ_I increases from zero (the SINAD increases), the PDF undergoes a metamorphosis from an exponential to an approximately Gaussian shape when $\mu_R^2\,\mu_I^2 >> \sigma^2$, the PDF of Y_m^2 can be approximated by Gaussian shape with a mean and variance

$$\mu_{Y_m^2}\approx\mu_R^2+\mu_I^2 \tag{22}$$

$$\sigma_{Y_m^2}^2\approx 2\sigma_\eta^2M\left(\mu_R^2+\mu_I^2\right) \tag{23}$$

The power spectral density $S(k)$ is equal to the magnitude squared of $Y(k)$ divided by M^2R, where R is the reference impedance

$$S(k)=\frac{[\mathrm{Re}(N(k))]^2+[\mathrm{Im}(N(k))]^2}{M^2R}=\frac{N_k^2}{M^2R} \tag{24}$$

Therefore, the PDF of S_m may be approximated by gaussian distribution, with mean and variance

$$\mu_{S_m}\approx\left(\mu_R^2+\mu_I^2\right)/M^2R \tag{25}$$

$$\sigma_{S_m}^2\approx 2\sigma_\eta^2\left(\mu_R^2+\mu_I^2\right)/M^3R \tag{26}$$

Or using Parseval's relation [6], we can show that

$$\mu_R^2+\mu_I^2=(A_xM/2)^2 \tag{27}$$

Then

$$\mu_{S_m}\approx\frac{A_x^2}{4R} \tag{28}$$

$$\sigma_{S_m}^2\approx\frac{\sigma_\eta^2A_x^2}{2R^2M} \tag{29}$$

The 95% confidence interval of the S_m is

$$\frac{A_x^2}{4R}-2\sqrt{\frac{\sigma_\eta^2}{R}\frac{A_x^2}{2RM}}\leq S_m\leq\frac{A_x^2}{4R}+2\sqrt{\frac{\sigma_\eta^2}{R}\frac{A_x^2}{2RM}} \tag{30}$$

Here, $S_m=A_x^2/4R$ is the PSD of the signal x for one side of two-sided Fourier Transform. Let us combine the signal power corresponding to both the positive and negative frequencies to obtain a familiar results for total signal power $\hat{P}_s=\sigma_s^2=A_x^2/2R$ Watts. The total noise power for all of the positive and negative frequencies of the entire FFT spectrum is $\hat{P}_\eta=\sigma_W^2=\sigma_\eta^2/R$ watts. After substituting these into (30), the relationship

$$\hat{P}_s-4\sqrt{\hat{P}_s\hat{P}_\eta/M}\leq P_s\leq\hat{P}_s+4\sqrt{\hat{P}_s\hat{P}_\eta/M} \tag{31}$$

can be derived as the 95% confidence interval of the signal power P_s.

4.2 Precision via digital filtering

4.2.1 PDF of digital Notch Filter Output

In this section we shall deal with the PDF of the sum of squares of the digital notch filter output in response of white noise. Consider an experiment where a signal plus white noise is applied to the input of the digital filter shown in Fig. 3. Let the center frequency f_r of the notch filter be exactly tuned to the signal frequency. The sine-wave will be filtered out with the result that only the noise emerges from the notch output X_{nt}. The noise emerging from the notch output will be correlated, but with a very sharp notch characteristic the noise will be nearly white and Gaussian. Thus as a fairly good approximation, we assume that the noise emerging from the notch output is white and Gaussian. So its Power Density Spectrum is given by:

$$S_\eta(f)=N^2/2 \tag{32}$$

If we integrate the true noise power over the bandwidth of interest, we obtain the total noise power which is

$$P_\eta=\int_{BW_m}S_\eta(f)df=N^2BW_m \tag{33}$$

Note that the total noise power is defined over a particular bandwidth, which in our case is BW_m. The power density spectrum of the noise emerging from the notch output is

$$\hat{S}_\eta(f)=|H_{nt}(f)|^2S_\eta(f) \tag{34}$$

This will be used as an estimate of the noise power. The total estimated noise power over the bandwidth BW_m is

$$\hat{P}_\eta=\int_{BWm}\hat{S}_\eta(f)df=\int_{BWm}|H_{nt}(f)|^2S_\eta(f)df \tag{35}$$

Recall that, from out initial assumption, the true white noise $S_\eta(f)$ is constant over all frequency so (35) reduces to

$$\hat{P}_\eta = N^2 \int_{BWm} |H_{nt}(f)|^2 df \tag{36}$$

Isolating the variable N^2 in (36) results in

$$N^2 = \frac{\hat{P}_\eta}{\int_{BWm} |H_{nt}(f)|^2 df} \tag{37}$$

This can be related to the true total noise power P_η in (33) as

$$P_\eta = N^2 BW_m = N^2 \frac{\hat{P}_\eta}{\int_{BW_m} |H_{nt}(f)|^2 df} \tag{38}$$

This equation make the relation between the true noise power and the measured noise power by digital filtering. Refer to Appendix A for the evaluation of the integral.

4.2.2 PDF of bandpass digital Filter Output

Let assume that, over the frequency range BW_m from $-F_s/2$ to $F_s/2$, the noise $\eta(n)$ is white with a power density spectrum $N^2/2$. Here, N is the level of noise expressed in $Volts/\sqrt{Hz}$. As described in the earlier section, the bandpass output of the digital filter will be used as an estimate of the signal power. The input signal to the bandpass filter is $y(n)=s(n)+\eta(n)$ where the signal $s(n)$ will be assumed to be single sine wave tone at the test frequency:

$$s(n) = A\cos(2\pi f_0 nT + \varphi) \tag{39}$$

Having a Power Density Spectrum

$$S_s(f) = \frac{A^2}{4}(\delta(f - f_0) + \delta(f + f_0)) \tag{40}$$

The noise signal $\eta(n)$ will be assumed to be zero-mean white noise, which has a Power Density Spectrum $S_\eta(n)=N^2/2$. From this, the Power Density Spectrum of the bandpass digital filter input $y(n)$ will be

$$S_y(f) = S_s(f) + S_\eta(f) = \frac{A^2}{4}(\delta(f - f_0) + \delta(f + f_0)) + \frac{N^2}{2} \tag{41}$$

The bandpass output of the digital filter has a frequency response $H_{bp}(f)$. The frequency interval over which the estimated signal power $\hat{P}_s$ will be calculated is BW_m, which ranges from $-F_s/2$ to $F_s/2$. The power Density Spectrum of the bandpass output is

$$\hat{S}_s(f) = S_s(f)|H_{bp}(f)|^2 + S_\eta(f)|H_{bp}(f)|^2 \tag{42}$$

The total power over the bandwidth of interest (BW_m) that is emerging from the bandpass output is

$$\begin{aligned} \hat{P}_s &= \int_{BW_m} \hat{S}_s(f) df \\ &= \int_{BW_m} S_s(f)|H_{bp}(f)|^2 df + \int_{BW_m} S_\eta(f)|H_{bp}(f)|^2 df \end{aligned} \tag{43}$$

But the desired signal $S_s(f)$ is known to be a pure tone, therefore (43) reduces to

$$\hat{P}_s = |H_{bp}(f_0)|^2 \frac{A^2}{2} + \int_{BW_m} S_\eta(f)|H_{bp}(f)|^2 df \tag{44}$$

We will first simplify (44) using the observation from (1) that the magnitude of the transfer function $H_{bp}(f)$ at the center frequency f_r is $|H_{bp}(f_r)| = 1$. The first term of the right-hand side of (44) is the true signal power P_s. Also, the Power Density Spectrum of the noise $S_\eta(f)$ is a constant $N^2/2$. We thus arrive at a relationship between the true signal power P_s and the estimated signal power $\hat{P}_s$:

$$\hat{P}_s = P_s + N^2 \int_{BW_m} |H_{bp}(f)|^2 df \tag{45}$$

The signal power as found from (45) will be used in most measurements that are accomplished using the digital filter. Refer to Appendix B for the evaluation of the integral.

4.2.3 Confidence Interval of signal power via digital filter

There is a bias in the estimated signal power as extracted by digital filter. The estimate, including the bias, is given by (45). We can assemble an empirical expression for an approximate 95% confidence interval of the true signal power based on (45) and (33).

An expression for the signal power which includes the bias and also accounts for the randomness of the noise is given by the following relationship

$$\begin{aligned} &\hat{P}_s - 4\sqrt{\hat{P}_s \hat{P}_\eta / M} - \hat{P}_\eta \int_{BW_m} |H_{bp}(f)|^2 df \\ &\qquad \le P_s \le \\ &\hat{P}_s + 4\sqrt{\hat{P}_s \hat{P}_\eta / M} - \hat{P}_\eta \int_{BW_m} |H_{bp}(f)|^2 df \end{aligned} \tag{46}$$

We will use this simple expression in our derivations for the confidence intervals of the various tests.

5. SIMULATION RESULTS

In order to explore the accuracy of this method, the proposed structure was simulated and the power spectral density is computed. The objective of our experiment is to compare the two different extraction schemes (FFT and filter bank). The circuit under test is a 60 MHz 10 bit CMOS pipelined ADC. The chip (THS1060) is a full custom proprietary Texas Instruments design. An input signal level of -0.5 dB was chosen. The test frequency was 4.999 MHz sampled at 50MHz. The acquisition is performed with the bench test CANTEST [7]. Then, the filter bank was tuned to track the input sine wave and the harmonics.

Table 1. Comparison of measured Signal Powers via FFT and Digital Filtering.

	FFT	Digital filtering
$P_{s,1}$	-0,50 dB	-0,49 dB
$P_{s,2}$	-84,34 dB	-84,44 dB
$P_{s,3}$	-64,60 dB	-64,67 dB
$P_{s,4}$	-86,01 dB	-85,98 dB
$P_{s,5}$	-77,62 dB	-77,65 dB
P_η	-55,24 dB	-55,30 dB

The estimated power spectral densities are slightly different than the value found from FFT, which indicates that the extraction via digital filter is valid, Table 1.

6. CONCLUSION

In this paper a filter bank scheme for on-chip signal tracking and power spectral density computation have been described. The presented theoretical development and simulation work has focused on the ADC testing.

7. APPENDIX A

Evaluation of the integral of the bandpass filter

Cauchy's Residue Theorem is used to evaluate the integral of the transfer function of the bandpass filter. The integral for the bandpass output is:

$$\int_{-F_s/2}^{+F_s/2} \left|H_{bp}(f)\right|^2 df = \frac{1}{2\pi jT} \oint_{|z|=1} \left(z^{-1} H_{bp}(z) H_{bp}\left(z^{-1}\right)\right) dz \qquad (47)$$

For the integrand on the right hand side of (47), the only poles which are inside the unit circle are at

$$z_{p1} = \frac{1}{2}\left(\left(2-k_2-k_1^2\right) + \sqrt{\left(2-k_2-k_1^2\right)^2 + 4\left(1-k_2\right)}\right) \qquad (48)$$

and

$$z_{p2} = \frac{1}{2}\left(\left(2-k_2-k_1^2\right) - \sqrt{\left(2-k_2-k_1^2\right)^2 + 4\left(1-k_2\right)}\right) \qquad (49)$$

and

$$z_{p2} = 0 \qquad (50)$$

From Cauchy's theorem, the integral is

$$\frac{1}{2\pi jT} \oint_{|z|=1} \left(z^{-1} H_{bp}(z) H_{bp}\left(z^{-1}\right)\right) dz = F_s\left(Res_{bp1} + Res_{bp2} + Res_{bp3}\right) \qquad (51)$$

where

$$Res_{bp1} = -\frac{k_2}{2z_{p1}} K_1 + K_1\left(\frac{K_1}{1-z_{p1}z_{p1}} + \frac{K_2}{1-z_{p2}z_{p1}}\right) \qquad (52)$$

$$Res_{bp2} = -\frac{k_2}{2z_{p2}} K_2 + K_2\left(\frac{K_1}{1-z_{p2}z_{p1}} + \frac{K_2}{1-z_{p2}z_{p2}}\right) \qquad (53)$$

$$Res_{bp3} = \frac{k_2}{2}\left(\frac{k_2}{2} + \frac{K_1}{z_{p1}} + \frac{K_2}{z_{p2}}\right) \qquad (54)$$

and

$$K_1 = -\frac{k_2}{2} \times \frac{\left(z_{p1}+1\right)\left(z_{p1}-1\right)}{z_{p1} - \frac{1}{2}\left(2-k_2-k_1^2\right) - \sqrt{\left(2-k_2-k_w^2\right)^2 - 4\left(1-k_1\right)}} \qquad (55)$$

$$K_2 = -\frac{k_2}{2} \times \frac{\left(z_{p1}+1\right)\left(z_{p1}-1\right)}{z_{p1} - \frac{1}{2}\left(2-k_2-k_1^2\right) + \sqrt{\left(2-k_2-k_1^2\right)^2 - 4\left(1-k_2\right)}} \qquad (56)$$

8. APPENDIX B

Evaluation of the integral of the notch filter

Similarly the integral for the notch filter is

$$\int_{-F_s/2}^{+F_s/2} \left|H_{nt}(f)\right|^2 df = \frac{1}{2\pi jT} \oint_{|z|=1} \left(z^{-1} H_{nt}(z) H_{nt}\left(z^{-1}\right)\right) dz \qquad (57)$$

The integrand in the right hand side of (57) has exactly the same poles as (47). Therefore the integral is

$$\frac{1}{2\pi jT} \oint_{|z|=1} \left(z^{-1} H_{nt}(z) H_{nt}\left(z^{-1}\right)\right) dz = F_s\left(Res_{nt1} + Res_{nt2} + Res_{nt3}\right) \qquad (58)$$

Where

$$Res_{nt1} = -\frac{2-k_2}{2z_{p1}} K_3 + K_3\left(\frac{K_3}{1-z_{p1}z_{p1}} + \frac{K_4}{1-z_{p2}z_{p1}}\right) \qquad (59)$$

$$Res_{nt2} = -\frac{2-k_2}{2z_{p2}} K_4 + K_4\left(\frac{K_3}{1-z_{p2}z_{p1}} + \frac{K_4}{1-z_{p2}z_{p2}}\right) \qquad (60)$$

$$Res_{bp3} = \frac{2-k_2}{2}\left(\frac{2-k_2}{2} + \frac{K_3}{z_{p1}} + \frac{K_4}{z_{p2}}\right) \qquad (61)$$

and

$$K_3 = \frac{2-k_2}{2} \times \frac{z_{p1}^2 - 2z_{p1}\frac{2-k_2-k_1^2}{2-k_2} + 1}{z_{p1} - \frac{1}{2}\left(2-k_2-k_1^2\right) - \sqrt{\left(2-k_2-k_1^2\right)^2 - 4\left(1-k_2\right)}} \qquad (62)$$

$$K_4 = \frac{2-k_2}{2} \times \frac{z_{p2}^2 - 2z_{p2}\frac{2-k_2-k_1^2}{2-k_2} + 1}{z_{p2} - \frac{1}{2}\left(2-k_2-k_1^2\right) - \sqrt{\left(2-k_2-k_1^2\right)^2 - 4\left(1-k_2\right)}} \qquad (63)$$

9. ACKNOWLEDGMENT

This work was supported by ST-Microelectronics Grenoble, Convention N° 01.2.93.1252: "new methods for ADC testing for dynamic measurement".

REFERENCES

[1] J. Doernberg, H. S. Lee, D. A. Hodges, "Full-Speed Testing of A/D Converters," *IEEE Journal Of Solid State Circuits,* Vol 19, N° 6, pp. 820-827, 1984.

[2] W. Martin, M. Padmanabhan, "Resonator based filter banks for frequency domain application," *IEEE Trans. On circuits and Systems-II*, Vol 38, N° 10, pp. 1145-1159, October 1991.

[3] M.F. Toner, G.W. Roberts, "A BIST scheme for an SNR, gain tracking, and frequency response test of a sigma-delta ADC," *IEEE Tran. on Circ. and Syst.-II*, Vol. 41, N° 12, pp. 1-15, Jan. 1995.

[4] P. Papoulis, "Probability, Random Variables, and Stochastic Process," McGraw-Hill, 1994.

[5] J. G. Proakis, "Digital Communications," McGraw-Hill, 1983.

[6] S. M. Kay, "Fundamentals of Statistical Signal Processing," Printice-Hall, 1993.

[7] D. Dallet, Y. Berthoumieu, "A survey on the dynamic characterization of A/D converters," *Journal of measurement,* Vol 24, pp. 263-279, 1998.

Authors: Ph.D. Student Chiheb REBAI, Assistant Professor Dominique DALLET and Professor Philippe MARCHEGAY, Laboratoire de Microélectronique IXL-ENSEIRB, Université Bordeaux I, 33405 Talence-Cedex France, Phone: +33 5 56 84 83 91, Fax: +33 5 56 37 15 45 , Email: rebai, dallet, marchegay@ixl.u-bordeaux.fr.